# Synthesis, Structures, and Properties of Bis($\mu$-oxo)nickel(III) and Bis($\mu$-superoxo)nickel(II) Complexes: An Unusual Conversion of a Ni$^{III}_2$($\mu$-O)$_2$ Core into a Ni$^{II}_2$($\mu$-OO)$_2$ Core by H$_2$O$_2$ and Oxygenation of Ligand

**Kazushi Shiren,[1a] Seiji Ogo,[1b] Shuhei Fujinami,[1a] Hideki Hayashi,[1a] Masatatsu Suzuki,\*,[1a] Akira Uehara,\*,[1a] Yoshihito Watanabe,\*,[1b] and Yoshihiko Moro-oka[1c]**

*Contribution from the Department of Chemistry, Faculty of Science, Kanazawa University, Kakuma-machi, Kanazawa, Ishikawa 920-1192, Japan, Institute for Molecular Science, Myodaiji, Okazaki 444-8585, Japan, and Research Laboratory of Resources Utilization, Tokyo Institute of Technology, 4259 Nagatsuta, Midori-ku, Yokohama 226-0026, Japan*

*Received February 1, 1999. Revised Manuscript Received July 7, 1999*

**Abstract:** A six-coordinate bis($\mu$-oxo)nickel(III) complex, [Ni$_2$($\mu$-O)$_2$(Me$_3$-tpa)$_2$]$^{2+}$ (**1**), was synthesized by the reaction of [Ni$_2$($\mu$-OH)$_2$(Me$_3$-tpa)$_2$]$^{2+}$ (**2**) with 1 equiv of hydrogen peroxide in methanol at −90 °C, where Me$_3$-tpa = tris(6-methyl-2-pyridylmethyl)amine. The 6-methyl groups of Me$_3$-tpa have a significant influence on the formation and stabilization of the high-valent bis($\mu$-oxo)dinickel(III) species. The reaction of **2** with a large excess of hydrogen peroxide (>10 equiv) afforded a novel bis($\mu$-superoxo)dinickel(II) complex, [Ni$_2$-($\mu$-O$_2$)$_2$(Me$_3$-tpa)$_2$]$^{2+}$ (**3**), thus, the reaction demonstrates a unique conversion of a Ni$^{III}$($\mu$-O)$_2$Ni$^{III}$ core into a Ni$^{II}$($\mu$-OO)$_2$Ni$^{II}$ core upon exposure to hydrogen peroxide. Complexes **1**, **2**, and **3** have been characterized by X-ray crystallography and various physicochemical techniques. Complex **1** has a Ni($\mu$-O)$_2$Ni core and the average Ni−O and Ni−N bond distances (1.871 and 2.143 Å, respectively) are significantly shorter than those of **2** (2.018 and 2.185 Å, respectively), suggesting that **1** is a bis($\mu$-oxo)dinickel(III) complex. Complex **3** consists of a Ni($\mu$-OO)$_2$Ni core with two $\mu$-1,2-O−O bridges to form a six-membered ring with chair conformation and the O−O bond distance is 1.345(6) Å. The resonance Raman spectrum of a powdered sample of **3** measured at ~110 K showed an isotope-sensitive band at 1096 cm$^{-1}$ (1044 cm$^{-1}$ for an $^{18}$O-labeled sample), indicating that **3** is a bis($\mu$-superoxo)dinickel(II) complex. Thermal decomposition of both **1** and **3** in acetone at −20 °C under N$_2$ atmosphere resulted in partial hydroxylation of a methyl group of Me$_3$-tpa in yields of 21−27% for both complexes. For complex **3**, a carboxylate complex, [Ni(Me$_2$-tpaCOO)(OH$_2$)]$^+$ (**4**), where one of the three methyl groups of Me$_3$-tpa is oxidized to carboxylate, was also isolated as a decomposed product under N$_2$ atmosphere. During the decomposition process of **3**, dioxygen evolution was simultaneously observed. The electrospray ionization mass spectrometry (ESI-MS) of **3** revealed the formation of **1** during the decomposition process. These results suggest that one possible decomposition pathway of **3** is a disproportionation of two coordinated superoxides to dioxygen and peroxide followed by the O−O bond scission of peroxide to regenerate **1**, which is responsible for the hydroxylation and the oxidation of the 6-methyl group of Me$_3$-tpa.

## Introduction

Dioxygen activation chemistry by metal complexes is of great importance for understanding the reaction mechanisms of dioxygen activating metalloproteins in biological systems and utilizing metal complexes as oxidation catalysts.[2] Recently, dioxygen activation by dimetal complexes has been shown to afford high-valent M$_2$($\mu$-O)$_2$ complexes (M = Cu,[3−13] Fe,[14−16] Co,[17,18] and Ni[17]) by the O−O bond scission of O$_2^{2-}$. For example, the O−O bond scission of ($\mu$-$\eta^2$:$\eta^2$-peroxo)dicopper-

(II) complexes having sterically hindered tridentate *N,N',N''*-trisubstitued tacn ligands[19] has been demonstrated to occur to

(1) (a) Kanazawa University. (b) Institute for Molecular Science. (c) Tokyo Institute of Technology.

(2) (a) Special thematic issue for Metal−Dioxygen Complexes: *Chem. Rev.* **1994**, *94*, 567−856 and references therein. (b) Special thematic issue for Oxygen Metabolism in Bioinorganic Enzymology: *Chem. Rev.* **1996**, *96*, 2541−2950 and references therein.

(3) (a) Mahapatra, S.; Halfen, J. A.; Wilkinson, E. C.; Pan, G.; Cramer, C. J.; Que, L., Jr.; Tolman, W. B. *J. Am. Chem. Soc.* **1995**, *117*, 8865−8866. (b) Mahapatra, S.; Halfen, J. A.; Wilkinson, E. C.; Pan, G.; Wang, X.; Young, V. G., Jr.; Cramer, C. J.; Que, L., Jr.; Tolman, W. B. *J. Am. Chem. Soc.* **1996**, *118*, 11555−11574.

(4) Halfen, J. A.; Mahapatra, S.; Wilkinson, E. C.; Kaderli, S.; Young, V. G., Jr.; Que, L., Jr.; Zuberbühler, A. D.; Tolman, W. B. *Science* **1996**, *271*, 1397−1400.

(5) Mahapatra, S.; Halfen, J. A.; Tolman, W. B. *J. Am. Chem. Soc.* **1996**, *118*, 11575−11586.

(6) (a) Mahapatra, S.; Kaderli, S.; Llobet, A.; Neuhold, Y.-M.; Palanché, T.; Halfen, J. A.; Young, V. G., Jr.; Kaden, T. A.; Que, L., Jr.; Zuberbühler, A. D.; Tolman, W. B. *Inorg. Chem.* **1997**, *36*, 6343−6356. (b) Mahapatra, S.; Young, V. G., Jr.; Kaderli, S.; Zuberbühler, A. D.; Tolman, W. B. *Angew. Chem., Int. Ed. Engl.* **1997**, *36*, 130−133.

(7) Tolman, W. B. *Acc. Chem. Res.* **1997**, *30*, 227−237 and references therein.

(8) Cole, A. P.; Root, D. E.; Mukherjee, P.; Solomon, E. I.; Stack, T. D. P. *Science* **1996**, *273*, 1848−1850.

(9) (a) Mahadevan, V.; Hou, Z.; Cole, A. P.; Root, D. E.; Lal, T. K.; Solomon, E. I.; Stack, T. D. P. *J. Am. Chem. Soc.* **1997**, *119*, 11996−11997. (b) DuBois, J. L.; Mukherjee, P.; Collier, A. M.; Mayer, J. M.; Solomon, E. I.; Hedman, B.; Stack, T. D. P.; Hodgson, K. O. *J. Am. Chem. Soc.* **1997**, *119*, 8578−8579.

(10) Allen, W. E.; Sorrell, T. N. *Inorg. Chem.* **1997**, *36*, 1732−1734.

produce bis(μ-oxo)dicopper(III) species, which show monooxygenase activity for ligand oxidation to give an *N*-dealkylated ligand and aldehyde or ketone upon thermal decomposition.[5] A similar observation was made for square planar bis(μ-oxo)-dicopper(III) complexes with sterically hindered bidentate *N,N,N′,N′*-tetrasubstituted cyclohexanediamines.[9] For diiron complexes, a bis(μ-oxo)diiron(IV) and a high-spin bis(μ-oxo)-diiron(III,IV) species have been generated by the reaction of $[Fe_2(\mu-O)_2(Me_3-tpa)_2]^{2+}$ with $H_2O_2$.[16b]

More recently, such high-valent metal-oxo chemistry has been extended to cobalt and nickel complexes; the reaction of $M^{II}_2$-(μ-OH)$_2$ complexes (M = Co or Ni) having sterically hindered hydrotris(pyrazolyl)borate derivatives with $H_2O_2$ produces five-coordinate bis(μ-oxo)dimetal(III) complexes, $[Ni^{III}_2$ or $Co^{III}_2$-(O)$_2(Tp^{Me3})_2]$ (**5** and **6**), which are active for ligand hydroxylation.[17] Despite the importance of such high-valent metal-oxo chemistry, there are only a limited number of well-characterized high-valent bis(μ-oxo)dimetal complexes as described above.

The structure and reactivity of metal complexes having reactive dioxygen intermediates such as $O_2^-$, $O_2^{2-}$, and $OOH^-$ are also interesting. Recently, a (μ-η²:η²-peroxo)dicopper(II) complex with a dinucleating polypyridyl ligand has been proposed to be a reactive intermediate for arene hydroxylation.[20] Thus it is important to explore how the nature and stereochemistry of ligands influence the formation, structures, and reactivity of high-valent metal-oxo complexes and/or complexes having reactive dioxygen intermediates with various metal ions.

A tetradentate tripodal ligand, Me₃-tpa, is useful for formation of bis(μ-oxo and/or hydroxo)dimetal cores,[21] since it can provide two vacant coordination sites in the cis-position. All the high-valent bis(μ-oxo)dimetal complexes mentioned above have ligands with sterically bulky substituents except for low-spin bis(μ-oxo)diiron(III,IV) complexes with tpa derivatives. Such ligands having sterically bulky substituents may provide a cavity for protecting a reactive high-valent bis(μ-oxo)dimetal center.

Such protection effect by a hydrophobic cavity has been proposed for diiron-peroxo model complexes.[22–24]

In this study, we report the syntheses of a six-coordinate bis-(μ-oxo)dinickel(III) complex, $[Ni^{III}_2(O)_2(Me_3-tpa)_2](BF_4)_2$, (**1**), and a bis(μ-superoxo)dinickel(II) complex, $[Ni^{II}_2(O_2)_2(Me_3-tpa)_2]$-$(BF_4)_2$ (**3**), having a sterically bulky tripodal tetradentate ligand, Me₃-tpa, by the reaction of $[Ni^{II}_2(\mu-OH)_2(Me_3-tpa)_2]^{2+}$ (**2**) with hydrogen peroxide in methanol at low temperature. Complex **3** is produced by an unprecedented conversion of a bis(μ-oxo)-dinickel(III) complex **1** upon exposure to $H_2O_2$. Complex **1** is the first six-coordinate bis(μ-oxo)dinickel(III) complex, although a five-coordinate bis(μ-oxo)dinickel(III) complex, $[Ni^{III}_2(O)_2$-$(Tp^{Me3})_2]$ (**5**), has been reported.[17] In addition, **3** is also the first structurally characterized bis(μ-superoxo)dinickel(II) complex. Hydroxylation and oxidation of a methyl group of Me₃-tpa by $Ni^{III}_2(\mu-O)_2$ center in **1** and the reactivity of **3** having two superoxides as an activated dioxygen intermediate are also presented.

## Experimental Section

**Materials**. Acetone was purified by distillation. 6-Methylpyridine-2-carbaldehyde was purified by distillation under a reduced pressure. Me₃-tpa was prepared as described previously.[25] $H_2^{18}O_2$ was prepared according to the literature.[26] Purity of $H_2^{18}O_2$ was checked by GC-MS (ca. 98%). All other reagents and solvents were commercially available and used without further purification.

**Syntheses of Complexes. [Ni₂(O)₂(Me₃-tpa)₂](BF₄)₂·6MeOH (1).** To a rapidly stirred solution of NiCl₂·6H₂O (59 mg, 0.25 mmol), Me₃-tpa (83 mg, 0.25 mmol), *n*-Bu₄NBF₄ (165 mg, 0.5 mmol), and 1 M *n*-Bu₄NOH in methanol (0.25 cm³, 0.25 mmol) in 50 cm³ of methanol at −90 °C was added dropwise 50 mM H₂O₂ in methanol (2.75 cm³, 0.14 mmol) over 2 h to produce a brown solution. The resulting solution was allowed to stand for 2 days at −80 °C to give **1** as brown crystals, which were suitable for X-ray crystallography. The complex decomposed even at −30 °C in solid state within a few minutes. UV−vis ($\lambda_{max}$/nm ($\epsilon$/M$^{-1}$ cm$^{-1}$) in acetone at −70 °C): 394 (∼4000). ESI-MS: *m/z* 913 [M − ClO₄]$^+$.

**[Ni₂(OH)₂(Me₃-tpa)₂](ClO₄)₂·(CH₃)₂CO (2).** To a mixture of Ni-(ClO₄)₂·6H₂O (183 mg, 0.50 mmol) and Me₃-tpa (166 mg, 0.50 mmol) in methanol/acetone (1:1) was added 1 M *n*-Bu₄NOH in methanol (0.5 cm³, 0.50 mmol) with stirring to produce a small amount of insoluble product, which was removed by filtration. The filtrate in a Schlenk tube was allowed to stand overnight under N₂ to afford **2** as light green crystals, which were characterized by X-ray crystallography. Calcd for C₄₅H₅₆N₈O₁₁Cl₂Ni₂ (**2**-ClO₄): C, 50.36; H, 5.26; N, 10.44; Ni, 10.94. Found: C, 50.13; H, 5.23; N, 10.62; Ni, 11.0. UV−vis ($\lambda_{max}$/nm ($\epsilon$/ M$^{-1}$ cm$^{-1}$) in methanol at −50 °C): 384 (190), 600 (50), 1184 (57). Molar conductivity: 74.8 Ω$^{-1}$ cm² mol$^{-1}$ at −78 °C in acetone.[27] IR (cm$^{-1}$): $\nu$(C=O), 1705; $\nu$(C=C), 1605; $\nu_3$(ClO₄), 1093. ESI-MS: *m/z* 915 [M − ClO₄]$^+$.

(11) Itoh, S.; Nakao, H.; Berreau, L. M.; Kondo, T.; Komatsu, M.; Fukuzumi, S. *J. Am. Chem. Soc.* **1998**, *120*, 2890−2899.

(12) Enomoto, M.; Aida, T. *J. Am. Chem. Soc.* **1999**, *121*, 874−875.

(13) Blain, I.; Bruno, P.; Giorgi, M.; Lojou, E.; Lexa, D.; Réglier, M. *Eur. J. Inorg. Chem.* **1998**, 1297−1304.

(14) Que, L., Jr. *J. Chem. Soc., Dalton Trans.* **1997**, 3933−3940.

(15) (a) Dong, Y.; Fujii, H.; Hendrich, M. P.; Leising, R. A.; Pan, G.; Randall, C. R.; Wilkinson, E. C.; Zang, Y.; Que, L., Jr.; Fox, B. G.; Kauffmann, K.; Münck, E. *J. Am. Chem. Soc.* **1995**, *117*, 2778−2792. (b) Kim, C.; Dong, Y.; Que, L., Jr. *J. Am. Chem. Soc.* **1997**, *119*, 3635−3636.

(16) (a) Dong, Y.; Que, L., Jr.; Kauffmann, K.; Münck, E. *J. Am. Chem. Soc.* **1995**, *117*, 11377−11378. (b) Dong, Y.; Zang, Y.; Shu, L.; Wilkinson, E. C.; Que, L., Jr.; Kauffmann, K.; Münck, E. *J. Am. Chem. Soc.* **1997**, *119*, 12683−12684.

(17) Hikichi, S.; Yoshizawa, M.; Sasakura, Y.; Akita, M.; Moro-oka, Y. *J. Am. Chem. Soc.* **1998**, *120*, 10567−10568.

(18) Hikichi, S.; Komatsuzaki, H.; Akita, M.; Moro-oka, Y. *J. Am. Chem. Soc.* **1998**, *120*, 4699−4710.

(19) Abbreviations of ligands used: Me₃-tpa = tris(6-methyl-2-pyridyl-methyl)amine; tpa = tris(2-pyridylmethyl)amine; Me-tpa = (6-methyl-2-pyridylmethyl)bis(2-pyridylmethyl)amine; Me₂-tpa = bis(6-methyl-2-pyridylmethyl)(2-pyridylmethyl)amine; Tp$^{Me_3}$ = hydrotris(3,4,5-trimethyl-1-pyrazolyl)borate; Tp$^{iPr,Me}$ = hydrotris(3-isopropyl-5-methyl-1-pyrazolyl)borate; tacn = 1,4,7-triazacyclononane; Me₃-tacn = 1,4,7-trimethyl-1,4,7-triazacyclononane; Bn₃-tacn = 1,4,7-tribenzyl-1,4,7-triazacyclononane; L$_{ME}$ = *N,N,N′,N′*-tetramethyl-(1R,2R)-cyclohexanediamine; Me₂-tpaCOOH = *N,N*-bis(6-methyl-2-pyridylmethyl)-6-aminomethylpyridine-2-carboxylic acid; Me₂-tpaOH = (6-hydroxymethyl-2-pyridylmethyl)bis(6-methyl-2-pyridylmethyl)amine.

(20) Pidcock, E.; Obias, H. V.; Zhang, C. X.; Karlin, K. D.; Solomon, E. I. *J. Am. Chem. Soc.* **1998**, *120*, 7841−7847.

(21) (a) Zang, Y.; Pan, G.; Que, L., Jr.; Fox, B. G.; Münck, E. *J. Am. Chem. Soc.* **1994**, *116*, 3653−3654. (b) Zang, Y.; Dong, Y.; Que, L., Jr.; Kauffmann, K.; Münck, E. *J. Am. Chem. Soc.* **1995**, *117*, 1169−1170. (c) Zheng, H.; Zang, Y.; Dong, Y.; Young, V. G., Jr.; Que, L., Jr. *J. Am. Chem. Soc.* **1999**, *121*, 2226−2235.

(22) (a) Kitajima, N.; Tamura, N.; Amagai, H.; Fukui, H.; Moro-oka, Y.; Mizutani, Y.; Kitagawa, T.; Mathur, R.; Heerwegh, K.; Reed, C. A.; Randall, C. R.; Que, L., Jr.; Tatsumi, K. *J. Am. Chem. Soc.* **1994**, *116*, 9071−9085. (b) Kim K.; Lippard, S. J. *J. Am. Chem. Soc.* **1996**, *118*, 4914−4915.

(23) (a) Dong, Y.; Ménage, S.; Brennan, B. A.; Elgren T. E.; Jang, H. G.; Pearce, L. L.; Que, L., Jr. *J. Am. Chem. Soc.* **1993**, *115*, 1851−1859. (b) Dong, Y.; Yan, S.; Young, V. G., Jr.; Que, L., Jr. *Angew. Chem., Int. Ed. Engl.* **1996**, *35*, 618−620.

(24) (a) Hayashi, Y.; Kayatani, T.; Sugimoto, H.; Suzuki, M.; Inomata, K.; Uehara, A.; Mizutani, Y.; Kitagawa, T.; Maeda, Y. *J. Am. Chem. Soc.* **1995**, *117*, 11220−11229. (b) Ookubo, T.; Sugimoto, H.; Nagayama, T.; Masuda, H.; Sato, T.; Tanaka, K.; Maeda, Y.; Okawa, H.; Hayashi, Y.; Uehara, A.; Suzuki, M. *J. Am. Chem. Soc.* **1996**, *118*, 701−702.

(25) Nagao, H.; Komeda, N.; Mukaida, M.; Suzuki, M.; Tanaka, K. *Inorg. Chem.* **1996**, *35*, 6809−6815.

(26) Sitter, A. J.; Terner J. *J. Label. Comp. Radiopharm.* **1985**, *22*, 461−465.

(27) The value is reported based on the concentration of the dimer. Further details are given in the Supporting Information.

**[Ni₂(O₂)₂(Me₃-tpa)₂](BF₄)₂·6MeOH (3).** Aqueous 30% $H_2O_2$ (0.50 cm³, 4.4 mmol) was added to a solution of $NiCl_2·6H_2O$ (119 mg, 0.5 mmol), Me₃-tpa (166 mg, 0.5 mmol), and 1 M *n*-Bu₄NOH in methanol (0.50 cm³, 0.5 mmol) in 25 cm³ of methanol at −60 °C to produce a dark brown solution. The resulting solution was allowed to stand overnight, to which a solution of *n*-Bu₄NBF₄ (230 mg, 0.7 mmol) in 5 cm³ of methanol was added. The resulting solution was left for a few days at −60 °C to give **3** as black crystals suitable for X-ray crystallography. The complex is thermally stable in the solid state for a few minutes at room temperature. (*Caution: The perchlorate salt of* **3** *exploded even under nitrogen atmosphere upon warming to room temperature and should be handled with care.*) UV−vis ($\lambda_{max}$/nm ($\epsilon$/ $M^{-1}$ cm$^{-1}$)) in acetone at −50 °C): 500 (∼280, shoulder), 600 (∼200, shoulder), 740 (123), 1108 (105). Resonance Raman (solid samples, ∼110 K): $\nu$(O−O), 1096 cm$^{-1}$ (1044 cm$^{-1}$ for $^{18}$O). ESI-MS (only a monomeric species was detected): *m/z* 422 [M/2 − BF₄]$^+$ (*m/z* 426 for $^{18}$O). Molar conductivity: 83.2 $\Omega^{-1}$ cm$^2$ mol$^{-1}$ at −78 °C in acetone.[27]

$^{18}$O-labeled **3** was prepared as follows. To a solution of $NiCl_2·6H_2O$ (48 mg, 0.2 mmol), Me₃-tpa (66 mg, 0.2 mmol), and 1 M *n*-Bu₄NOH in methanol (0.20 cm³, 0.2 mmol) in 3 cm³ of methanol at −80 °C was added $H_2^{18}O_2$, which was prepared by dehydration of 3 cm³ of methanol solution containing 1.5 cm³ of 1% aqueous $H_2^{18}O_2$ (0.4 mmol) by anhydrous $Na_2SO_4$ (10 g), to produce a dark brown solution. After 1 h, *n*-Bu₄NClO₄ (102 mg, 0.3 mmol) in 1 cm³ of methanol was added to the solution. The resulting solution was allowed to stand for 1 day at −80 °C to give labeled **3** as a dark brown powder.

**[Ni(Me₂-tpaCOO)(OH₂)]ClO₄ (4).** Thermal decomposition of **3** (ca. 100 mg) in 100 cm³ of acetone at −20 °C under $O_2$ atmosphere afforded a green powder within 2 h. Although the Fast Atom Bombardment (FAB) mass spectrum of the green powder suggested the presence of [Ni(Me₂-tpaCOO)]$^+$, **4** could not be isolated by recrystallization from common organic solvents. Purification was achieved as follows. The green powder was dissolved into acetone (10 cm³) and then 14% aqueous $NH_4OH$ (20 cm³) was added and the organic layer was removed by extraction with $CHCl_3$ (30 cm³). The resulting aqueous solution was allowed to stand for several days to give **4** as green crystals suitable for X-ray crystallography. Calcd for $C_{21}H_{23}N_4O_7ClNi$: C, 46.92; H, 4.31; N, 10.42; Ni, 10.92. Found: C, 46.75; H, 4.32; N, 10.62; Ni, 11.1. IR (cm$^{-1}$): $\nu$(C=C), 1606; $\nu_{as}$(COO), 1579; $\nu_s$(COO), 1394; $\nu_3$(ClO₄), 1090. FAB-MS: Calcd for $C_{21}H_{21}N_4O_2Ni$ ([M − H₂O − ClO₄]$^+$) *m/z* 419.1018; found *m/z* 419.1051.

**Physical Measurements.** Electronic spectra were measured on a Hitachi U-3400 spectrophotometer, and for low-temperature measurements, an Otsuka Denshi optical glass fiber attachment was used. Infrared spectra were obtained by the KBr-disk method with a HORIBA FT-200 spectrophotometer. $^1$H NMR spectra were measured on a JEOL GX 400 spectrometer. Quantitative analysis of nickel ion was carried out by a Hitachi Z-6100 polarized Zeeman atomic absorption spectrophotometer. The molar conductivities were measured at −78 °C in acetone (ca. 1 × 10$^{-3}$ M) with a TOA CM-20S conductivity meter. GC-MS analyses were performed on a Shimadzu GCMS-QP5000 GC-MS equipped with a Shimadzu fused silica capillary column HiCap-CBP1-M25-025 (0.22 mm diameter × 25 m).

ESI mass spectra were obtained with an API 300 triple quadruple mass spectrometer (PE-Sciex) in positive ion detection mode, equipped with an ion spray interface. The sprayer was held at a potential of 4.5 kV and compressed $N_2$ was employed to assist liquid nebulization. Orifice potential was maintained at 25 V.

Resonance Raman spectra were obtained by a JASCO R-500 laser Raman spectrophotometer. Resonance Raman samples of **3** were prepared by finely grinding the wet solids with methanol in an EPR tube (4 mm i.d.) with use of a brass rod in liquid $N_2$−methanol bath. The EPR tube containing sample was transferred into a cryostat that was cooled to ∼110 K by cold nitrogen flow generated by evaporation of liquid $N_2$. Raman scattering was excited at 488.0 nm (100 mW) with a Ar−Ion laser and collected using an approximately 140° backscattering geometry. Raman shifts were referenced to a band at 983 cm$^{-1}$ of $K_2SO_4$.

**Isolation and Identification of Modified Ligands by Thermal Decomposition of 1 and 3. Thermal Decomposition of 1.** Thermal

decomposition was performed under both $N_2$ and $O_2$ atmosphere. Since it was difficult to weigh the amount of **1** due to its thermal instability, the amounts used for the experiments were determined as follows. Typically, **1** (ca. 100 mg) was dissolved into 90 cm³ of acetone at −80 °C. The resulting solution was warmed to −20 °C and allowed to stand for 2 h to produce a blue-green solution under $N_2$ atmosphere (a blue-green suspension under $O_2$ atmosphere). After warming to room temperature, the suspension was made clear by adding water and then the volume of the resulting solution was adjusted to 100 cm³ in a volumetric flask with water. A portion (1.00 cm³) was taken up and the concentration of nickel ion was determined by atomic absorption spectrophotometry. Isolation and quantitative analysis for Me₃-tpa, Me₂-tpaOH, and Me₂-tpaCOO$^-$ were as follows. A solution of KCN (107 mg, ∼20 equiv) in 100 cm³ of water was added to the above remaining solution and then $CHCl_3$ (200 mL) was added to extract an organic layer containing Me₃-tpa and its oxidized products except for Me₂-tpaCOO$^-$. The aqueous layer was extracted three times with 100 cm³ of $CHCl_3$. The combined extract was dried over $Na_2SO_4$ and the solvent was removed under reduced pressure to give a yellow oil. The amounts of Me₃-tpa and Me₂-tpaOH were determined by $^1$H NMR by addition of a known amount of 1,4,7,10-tetraazacy-clododecane (cyclen) as an internal standard. The aqueous layer was evaporated to dryness under reduced pressure. The residue was dissolved into $D_2O$. The amount of Me₂-tpaCOO$^-$ was determined by $^1$H NMR.

Total amounts of Me₃-tpa, Me₂-tpaOH, and Me₂-tpaCOO$^-$ recovered were 89 ± 2% for three experiments. Yields of Me₂-tpaOH and Me₂-tpaCOO$^-$ under $N_2$ atmosphere were 24 ± 3% and 0%, respectively, based on a dimer. Hereafter yields are reported based on a dimer. Those under $O_2$ atmosphere were 13 ± 2% and 24 ± 3%, respectively.

Me₂-tpaOH was isolated by silica gel column chromatography and identified by $^1$H NMR and MS. $^1$H NMR ($CDCl_3$, 400 MHz reference to TMS): $\delta$ 7.63 (1H, t, py), 7.55 (2H, t, py), 7.44 (2H, d, py), 7.43 (1H, d, py), 7.05 (1H, d, py), 7.00 (2H, d, py), 4.72 (2H, s, pyC*H₂*-OH), 3.88 (2H, s, NC*H₂*py), 3.86 (4H, s, NC*H₂*py), 2.53 (6H, s, CH₃). EI-MS: calcd for $C_{21}H_{24}N_4O$ (M$^+$) *m/z* 348.1950; found *m/z* 348.1957.

Identification of Me₂-tpaCOO$^-$ was carried out by $^1$H NMR and FAB MS. $^1$H NMR ($D_2O$, 400 MHz, pD = ca. 12): $\delta$ 7.71 (1H, t, py), 7.61 (1H, d, py), 7.56 (2H, t, py), 7.47 (1H, d, py), 7.25 (2H, d, py), 7.05 (2H, d, py), 3.87 (2H, s, NC*H₂*py), 3.81 (4H, s, NC*H₂*py), 2.39 (6H, s, CH₃). FAB-MS: calcd for $C_{21}H_{21}N_4O_2$ (M$^-$) *m/z* 361.1665; found *m/z* 361.1664.

**Thermal Decomposition of 3.** Thermal decomposition was also conducted under both $N_2$ and $O_2$ atmosphere. Solid samples of **3** (typically ca. 100 mg) were quickly weighed at room temperature on an analytical balance and dissolved into 100 cm³ of acetone at −50 °C under $N_2$ atmosphere. The resulting solution was warmed to −20 °C and allowed to stand for 2 h to produce a blue-green suspension. After warming to room temperature, isolation and quantitative analysis for Me₃-tpa, Me₂-tpaOH, and Me₂-tpaCOO$^-$ were carried out by the same manner as those for **1**.

Total amounts of Me₃-tpa, Me₂-tpaOH, and Me₂-tpaCOO$^-$ recovered were 89 ± 3% for two experiments. Yields of Me₂-tpaOH and Me₂-tpaCOO$^-$ under $N_2$ atmosphere were 24 ± 3% and 12 ± 3%, respectively. Thermal decomposition under $O_2$ atmosphere gave 13 ± 2% of Me₂-tpaOH and 25 ± 4% of Me₂-tpaCOO$^-$.

**Dioxygen Evolution Analysis.** The amount of dioxygen was measured on a Shimadzu GC-8A gas chromatograph equipped with a TCD detector with a 3 m column (2.6 mm i.d.) of molecular sieve 5A (30−60 mesh). A weighed amount of **3** (50−100 mg) was dissolved in 10 cm³ of acetone in a Schlenk tube (ca. 25 cm³) at −50 °C under Ar atmosphere. Then it was warmed to 0 °C. After decomposition of **3**, the amount of dioxygen evolved was determined by GC. The amount of dioxygen was calibrated by injecting the appropriate amounts of $O_2$ gas under the same conditions without **3**. Yield: 35 ± 4% based on a dimer for three experiments.

**X-ray Crystallography. General Procedures.** Data were collected on a Rigaku RAXIS-IV imaging plate area detector using graphite monochromated Mo K$\alpha$ radiation ($\lambda$ = 0.71070 Å). Crystal-to-detector distance was 120 mm. To determine the cell constants[28] and the orientation matrix, three oscillation photographs were taken with an

**Table 1.** Crystallographic Data for $[Ni_2(O)_2(Me_3-tpa)_2](BF_4)_2 \cdot 6CH_3OH$ (**1**), $[Ni_2(OH)_2(Me_3-tpa)_2](ClO_4)_2 \cdot CH_3COCH_3$ (**2**), $[Ni_2(O_2)_2(Me_3-tpa)_2](BF_4)_2 \cdot 6CH_3OH$ (**3**), and $[Ni(Me_2-tpaCOO)(OH_2)]ClO_4$ (**4**)

|  | **1** | **2** | **3** | **4** |
|---|---|---|---|---|
| formula | $C_{48}H_{72}N_8O_8B_2F_8Ni_2$ | $C_{45}H_{56}N_8O_{11}Cl_2Ni_2$ | $C_{48}H_{72}N_8O_{10}B_2F_8Ni_2$ | $C_{21}H_{23}N_4O_7ClNi$ |
| temp, °C | −120 | −116 | −116 | 23 |
| MW | 1180.15 | 1073.29 | 1212.15 | 537.59 |
| cryst system | orthorhombic | triclinic | monoclinic | monoclinic |
| space group | $Pccn$ | $P\bar{1}$ | $P2_1/n$ | $P2_1/c$ |
| $a$, Å | 14.491(5) | 12.916(3) | 13.301(6) | 11.629(2) |
| $b$, Å | 16.422(4) | 17.394(3) | 15.638(8) | 12.968(2) |
| $c$, Å | 23.392(8) | 11.700(3) | 13.857(4) | 16.396(2) |
| $\alpha$, deg | 90 | 107.22(2) | 90 | 90 |
| $\beta$, deg | 90 | 108.63(2) | 104.17(2) | 109.840(9) |
| $\gamma$, deg | 90 | 84.53(2) | 90 | 90 |
| $V$, Å$^3$ | 5566(2) | 2379.1(10) | 2795(2) | 2325.8(5) |
| $Z$ | 4 | 2 | 2 | 4 |
| $2\theta_{max}$ | 51.3 | 51.7 | 51.3 | 51.4 |
| $F(000)$ | 2472.0 | 1120.0 | 1268.0 | 1112.0 |
| $D_{calcd}$, g/cm$^3$ | 1.408 | 1.498 | 1.440 | 1.535 |
| abs coeff, cm$^{-1}$ | 7.60 | 9.72 | 7.62 | 9.99 |
| no. of reflcns collcd | 4295 | 8206 | 4544 | 3970 |
| no. of indpt reflcns | 2673 ($I \geq 3\sigma(I)$) | 7510 ($I \geq 3\sigma(I)$) | 3386 ($I \geq 3\sigma(I)$) | 3185 ($I \geq 3\sigma(I)$) |
| no. of refined params | 329 | 614 | 353 | 308 |
| GOF | 2.43 | 1.65 | 1.68 | 1.62 |
| largest peak/hole, e Å$^{-3}$ | 0.59/−0.80 | 1.00/−0.95 | 1.02/−0.70 | 0.59/−0.64 |
| $R^a$ | 0.096 | 0.056 | 0.084 | 0.059 |
| $R_w$ | 0.130$^b$ | 0.096$^c$ | 0.122$^d$ | 0.087$^e$ |

$^a$ $R = \sum[|F_o| - |F_c|]/\sum|F_o|$. $^b$ $R_w = [\sum w(|F_o| - |F_c|)^2/\sum w|F_o|^2]^{1/2}$; $w = 1/[\sigma^2(F_o) + p^2|F_o|^2/4]$ ($p = 0.068$). $^c$ $R_w = [\sum w(|F_o| - |F_c|)^2/\sum w|F_o|^2]^{1/2}$; $w = 1/[\sigma^2(F_o) + p^2|F_o|^2/4]$ ($p = 0.098$). $^d$ $R_w = [\sum w(|F_o| - |F_c|)^2/\sum w|F_o|^2]^{1/2}$; $w = 1/[\sigma^2(F_o) + p^2|F_o|^2/4]$ ($p = 0.095$). $^e$ $R_w = [\sum w(|F_o| - |F_c|)^2/\sum w|F_o|^2]^{1/2}$; $w = 1/[\sigma^2(F_o) + p^2|F_o|^2/4]$ ($p = 0.076$).

oscillation angle of 2°. Intensity data were collected by taking oscillation photographs. The data were corrected for Lorentz and polarization effects, but not for the absorption effect.

The structures were solved by a direct method (SHELXS-86)[29] and expanded using a Fourier technique.[30] The structures were refined by a full-matrix least-squares method by using the teXsan[31] crystallographic software package (Molecular Structure Corporation). Hydrogen atoms were positioned at calculated positions. They were included, but not refined, in the final least-squares cycles.

Crystallographic data are summarized in Table 1. Tables of final atomic coordinates, thermal parameters, and full bond distances and angles are given in the Supporting Information.

**$[Ni_2(O)_2(Me_3-tpa)_2](BF_4)_2 \cdot 6CH_3OH$ (1).** A single crystal with dimensions of $0.30 \times 0.20 \times 0.05$ mm was picked up on a handmade cold copper plate mounted inside a liquid $N_2$ Dewar vessel and mounted on a glass rod at ca. −80 °C. Intensity data were collected by taking 37 oscillation photographs (total oscillation range 74°; oscillation angle 2°; exposure time 6 min).

The asymmetric unit is comprised of half of an $[Ni_2(O)_2(Me_3-tpa)_2]^{2+}$ ion along with one $BF_4^-$ ion and three methanol molecules. All non-hydrogen atoms were refined with anisotropic displacement parameters except for methanol molecules. Three methanol molecules were refined with disordered models with isotropic displacement parameters. The maximum shift was 0.02 in the final least-squares cycles. The final $R$ and $R_w$ values were 0.096 and 0.130, respectively.

**$[Ni_2(OH)_2(Me_3-tpa)_2](ClO_4)_2 \cdot (CH_3)_2CO$ (2).** A single crystal ($0.60 \times 0.40 \times 0.30$ mm) was picked up at room temperature and mounted on a glass rod. Intensity data were collected by taking 39 oscillation photographs (total oscillation range 156°; oscillation angle 4°; exposure time 22 min).

(28) The unit-cell parameters for **2** and **4** were also determined by least-squares calculations for 25 reflections on the setting angles with 22.93° < $2\theta$ < 29.53° and 25.36° < $2\theta$ < 29.31° that were collected on a Rigaku AFC-7R four circle automated diffractometer. The parameters obtained are in agreement with those obtained from IP measurement within standard deviations.

(29) G. M. Sheldrick, SHELXS-86; A Program for Crystal Structure Determination; University of Göttingen, FRG, 1986.

(30) Beurskens, P. T.; Admiraal, G.; Beurskens, G.; Bosman, W. P.; de Gelder, R.; Israel, R.; Smits, J. M. M. The DIRDIF-94 program system 1994, Technical Report of the Crystallography Laboratory, University of Nijmegen, The Netherlands.

The asymmetric unit consists of two halves of $[Ni_2(OH)_2(Me_3-tpa)_2]^{2+}$ ions, two $BF_4^-$ ions, and an acetone molecule. The structures of two cations are almost mirror images of each other. All non-hydrogen atoms were refined with anisotropic displacement parameters. The maximum shift was 0.00 in the final least-squares cycles. The final $R$ and $R_w$ values were 0.056 and 0.096, respectively.

**$[Ni_2(O_2)_2(Me_3-tpa)_2](BF_4)_2 \cdot 6CH_3OH$ (3).** A single crystal ($0.60 \times 0.50 \times 0.40$ mm) was picked up and mounted on a glass rod at ca. −80 °C. Intensity data were collected by taking 53 oscillation photographs (total oscillation range 106°; oscillation angle 2°; exposure time 6 min).

The asymmetric unit is comprised of half of an $[Ni_2(O_2)_2(Me_3-tpa)_2]^{2+}$ ion along with a $BF_4^-$ ion and three methanol molecules. All non-hydrogen atoms were refined anisotropically. The maximum shift was 0.00 in the final least-squares cycles. The final values of $R$ and $R_w$ were 0.084 and 0.122, respectively.

**$[Ni(Me_2-tpaCOO)(OH_2)]ClO_4$ (4).** A single crystal with dimensions of $0.3 \times 0.15 \times 0.15$ mm was mounted on a glass rod at room temperature. Intensity data were collected by taking 40 oscillation photographs (total oscillation range 160°; oscillation angle 4°; exposure time 20 min).

The asymmetric unit consists of an $[Ni(Me_2-tpaCOO)(OH_2)]^+$ ion and a $ClO_4^-$ ion. All non-hydrogen atoms were refined with anisotropic displacement parameters. The maximum shift was 0.00 in the final least-squares cycles. The final $R$ and $R_w$ values were 0.059 and 0.087, respectively.

## Results

**Synthesis of Complexes**. For preparation of **1** and **3**, the concentration and stoichiometry of the reactants, **2** and hydrogen peroxide, are of key importance. Complex **1** was obtained only under the conditions where the concentrations of a methanol solution of **2** and a methanol solution of hydrogen peroxide are less than 3 and 50 mM, respectively, and an equimolar amount of hydrogen peroxide was added very slowly over 2 h below −90 °C. Addition of an excess of hydrogen peroxide (more than 3 equiv) caused a color change from brown to blue-green

(31) teXsan: Crystal Structure Analysis Package, Molecular Structure Corporation, 1985 and 1992.
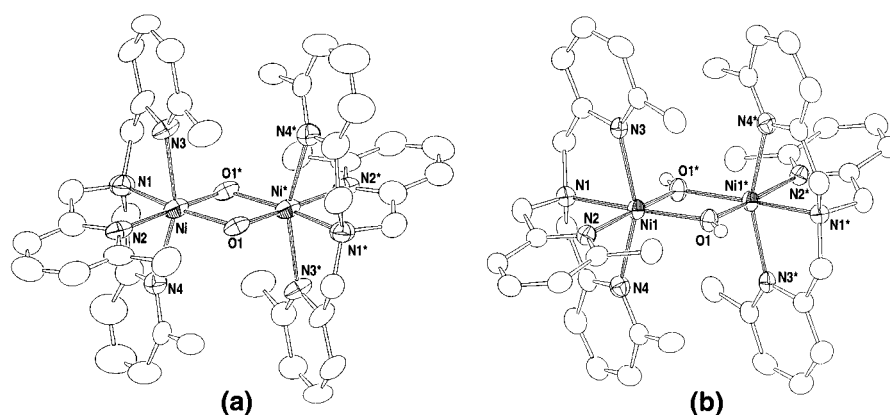
**Figure 1.** ORTEP views (50% probability) of complex cations of **1** (a) and **2** (b). Hydrogen atoms are omitted for clarity.

**Table 2.** Setected Bond Distances (Å) and Angles (deg) of [Ni$_2$(O)$_2$(Me$_3$-tpa)$_2$](BF$_4$)$_2$·6CH$_3$OH (**1**), [Ni$_2$(OH)$_2$(Me$_3$-tpa)$_2$](ClO$_4$)$_2$·CH$_3$COCH$_3$ (**2**), [Ni$_2$(O$_2$)$_2$(Me$_3$-tpa)$_2$](BF$_4$)$_2$·6CH$_3$OH (**3**), and [Ni(Me$_2$-tpaCOO)(OH$_2$)]ClO$_4$ (**4**)

| **1** | | **2** | | | | **3** | | **4** | |
|---|---|---|---|---|---|---|---|---|---|
| | | | | Bond Distances (Å) | | | | | |
| Ni−O | 1.888(6) | Ni1−O1 | 2.003(2) | Ni2−O2 | 1.998(3) | Ni−O1 | 1.956(5) | Ni−O1 | 2.084(4) |
| Ni−O* | 1.854(7) | Ni1−O1* | 2.033(2) | Ni2−O2* | 2.036(3) | Ni−O2* | 1.969(5) | Ni−O3 | 2.016(3) |
| Ni−N1 | 2.019(8) | Ni1−N1 | 2.089(3) | Ni2−N5 | 2.096(3) | Ni−N1 | 2.047(6) | Ni−N1 | 2.119(4) |
| Ni−N2 | 2.045(9) | Ni1−N2 | 2.142(3) | Ni2−N6 | 2.144(3) | Ni−N2 | 2.096(6) | Ni−N2 | 1.972(4) |
| Ni−N3 | 2.220(8) | Ni1−N3 | 2.241(3) | Ni2−N7 | 2.204(3) | Ni−N3 | 2.240(5) | Ni−N3 | 2.196(4) |
| Ni−N4 | 2.288(8) | Ni1−N4 | 2.251(3) | Ni2−N8 | 2.309(3) | Ni−N4 | 2.177(6) | Ni−N4 | 2.238(4) |
| Ni⋯Ni* | 2.924(1) | Ni1⋯Ni1* | 3.090(1) | Ni2⋯Ni2* | 3.091(1) | Ni⋯Ni* | 3.924(2) | | |
| O⋯O* | 2.334(6) | O1⋯O1* | 2.596(3) | O2⋯O2* | 2.592(4) | O1−O2 | 1.345(6) | | |
| | | | | Bond Angles (deg) | | | | | |
| O−Ni−O* | 77.2(3) | O1−Ni1−O1* | 80.1(1) | O2−Ni2−O2* | 79.9(1) | O1−Ni−O2* | 78.8(2) | | |
| Ni−O−Ni* | 102.8(3) | Ni1−O1−Ni1* | 99.9(1) | Ni2−O2−Ni2* | 100.1(1) | Ni−O1−O2 | 113.0(4) | | |
| | | | | | | Ni−O2*−O1* | 116.1(3) | | |

and no isolable compound was obtained. Such a color change suggests that hydrogen peroxide reacts with **1** to reduce Ni(III) to Ni(II) ion under the reaction conditions. Complex **1** is thermally unstable and decomposed even at −30 °C in solid state within a few minutes to give green compounds.

In contrast, **3** was obtained by treating a concentrated methanol solution of **2** (more than 10 mM) with an excess of 30% H$_2$O$_2$ (more than 10 equiv). Complex **3** is relatively stable in solid state compared with **1**.

We have attempted to prepare a series of bis($\mu$-oxo)dinickel-(III) complexes having less sterically bulky ligands, tpa, Me-tpa, and Me$_2$-tpa, by the method used for **1**. In the case of tpa and Me-tpa, the reaction with H$_2$O$_2$ did not show any distinct color changes, implying that a detectable amount of bis($\mu$-oxo)-dinickel(III) species is not produced. In the case of Me$_2$-tpa, distinct brown color was observed upon the reaction with H$_2$O$_2$, but it disappeared within a few seconds. Thus the set of three methyl groups of Me$_3$-tpa plays an essential role for the formation and stabilization of the bis($\mu$-oxo)dinickel(III) species.

**Structure Description of 1, 2, 3, and 4.** Figure 1a shows the crystal structure of a complex cation of **1** which consists of a Ni$_2$($\mu$-O)$_2$ core with Me$_3$-tpa nitrogens as found for [Fe$_2$(O)$_2$-(Me$_3$-tpa)$_2$]$^{2+}$ by Que et al.[21b] The selected bond distances and angles of **1** are given in Table 2. The nickel atoms adopt a distorted octahedral structure. The average Ni−O and Ni−N bond distances (1.871 and 2.143 Å) and the Ni⋯Ni$^*$ separation (2.924(1) Å) of **1** are significantly shorter than those of **2** (2.018, 2.185, and 3.091 Å, respectively, in Table 2 and Figure 1b). The average Ni−O bond distance and the Ni⋯Ni$^*$ separation is slightly longer than those in [Ni$^{III}$$_2$(O)$_2$(Tp$^{Me3}$)$_2$] (**5**; 1.856 and 2.882(3) Å, respectively), whereas the average Ni−N bond distance is substantially longer than that of **5** (2.012 Å) reported

by Hikichi et al.[17] A comparison of the bond distances suggests that **1** is also a bis($\mu$-oxo)dinickel(III) complex as **5**. The average Ni−N(axial) bond distance (2.254 Å) is significantly longer than the average Ni−N(equatorial) bond distance (2.032 Å), in line with the observation made for **5**. This elongation of the axial bonds appears to be attributable to the Jahn−Teller effect arising from a low-spin d$^7$ electron configuration. Elongation of the Ni−O and Ni−N bonds in **1** compared with those in **5** seems to be due to weaker Lewis acidity of the six-coordinate Ni(III) centers in **1** relative to that of the five-coordinate Ni(III) centers in **5** and/or an unfavorable steric interaction between the 6-methyl groups of Me$_3$-tpa and the oxo groups as found for the related compounds with the 6-methylpyridyl groups.[21,24a,25,32,33]

Such elongation of the Ni−N bond distances arising from the steric requirement of the 6-methylpyridyl groups is clearly observed in **2** (Table 2 and Figure 1b). The average Ni−N(6-methylpyridyl) bond distance (2.215 Å) in **2** is significantly longer than the Ni−N(pyridyl) bond distance of [Ni$_2$($\mu$-OH)$_2$-(tpa)$_2$]$^{2+}$ (**7**; 2.107 Å).[34] Thus the introduction of a methyl group into the 6-position of the pyridyl group causes a substantial elongation of the Ni−N(6-methylpyridyl) bonds compared with the Ni−N(pyridyl) bonds. In contrast, the Ni−N1(tertiary amine) bond distance in **2** (2.093 Å) is slightly shorter than that of **7** (2.114 Å), which may partially compensate the elongation of the Ni−N(6-methylpyridyl) bond.

(32) (a) Goodson, P. A.; Hodgson, D. J. *Inorg. Chem.* **1989**, *28*, 3606−3608. (b) Goodson, P. A.; Oki, A. R.; Glerup, J.; Hodgson, D. J. *J. Am. Chem. Soc.* **1990**, *112*, 6248−6254.

(33) Zang, Y.; Kim, J.; Dong, Y.; Wilkinson, E. C.; Appelman, E. H.; Que, L., Jr. *J. Am. Chem. Soc.* **1997**, *119*, 4197−4205.

(34) Ito, M.; Sakai, K.; Tsubomura, T.; Takita, Y. *Bull. Chem. Soc. Jpn.* **1999**, *72*, 239−247.
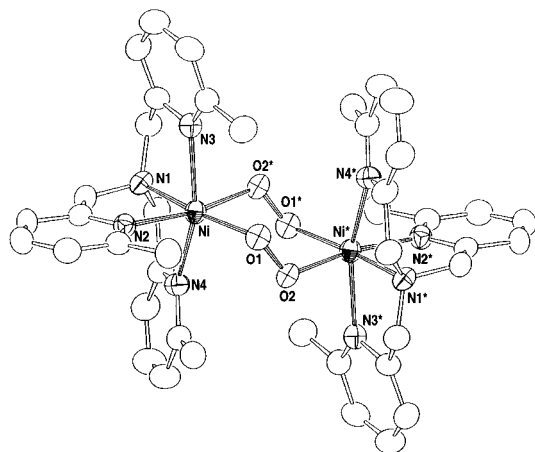
**Figure 2.** ORTEP view (50% probability) of a complex cation of **3**. Hydrogen atoms are omitted for clarity.
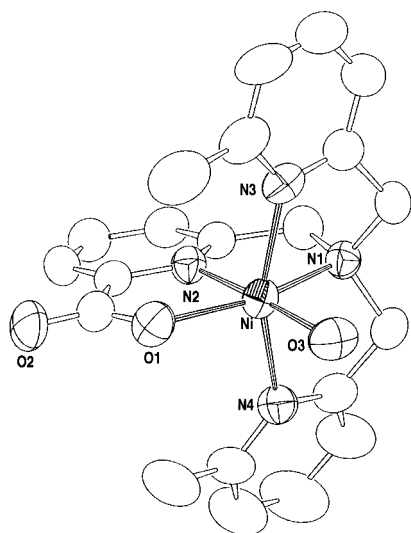


**Figure 3.** ORTEP view (50% probability) of a complex cation of **4**. Hydrogen atoms are omitted for clarity.

The crystal structure of **3** consists of a centrosymmetric Ni-$(\mu\text{-OO})_2$Ni core with $Me_3$-tpa nitrogens (Table 2 and Figure 2). The nickel centers in distorted octahedral structure are linked by two $\mu$-1,2-O−O bridges to form a six-membered ring with chair conformation having a Ni−O−O−Ni torsion angle of 91.6°. Such a M($\mu$-O−O)$_2$M structure also has been found in the bis($\mu$-superoxo) complexes, $[Co^{II}_2(O_2)_2(Tp^{iPr,Me})_2]$ (**8**)[35] and $[Co^{II,III}_2(O_2)_2(OH)(Me_3\text{-tacn})_2]^{2+}$ (a boat conformation),[36] and a bis($\mu$-peroxo) complex, $[Pt^{IV}_2Cl_2(O_2)_2(tacn)_2]^{2+}$.[37] The average Ni−O bond distance of **3** (1.963 Å) is significantly longer than that of **1** (1.871 Å), but shorter than that of **2** (2.018 Å). The O−O bond distance (1.345(6) Å) is comparable to that of **8** (1.354(5) Å),[35] which is between those of the peroxo and superoxo complexes.[38] Resonance Raman spectra of **3** confirmed the presence of superoxide (vide infra).

Figure 3 shows the crystal structure of **4**. The nickel atom is in a distorted octahedral structure with a pentadentate $Me_2$-tpaCOO$^-$ and a water molecule. The structure clearly shows that one of the methyl groups in $Me_3$-tpa is oxidized to carboxylate (vide infra).

(35) Reinaud, O. M.; Yap, G. P. A.; Rheingold, A. L.; Theopold, K. H. *Angew. Chem., Int. Ed. Engl.* **1995**, *34*, 2051−2052.
(36) Hayashi, Y.; Obata, M.; Suzuki, M.; Uehara, A. *Chem. Lett.* **1997**, 1255−1256.
(37) Davies, M. S.; Hambley, T. W. *Inorg. Chem.* **1998**, *37*, 5408−5409.
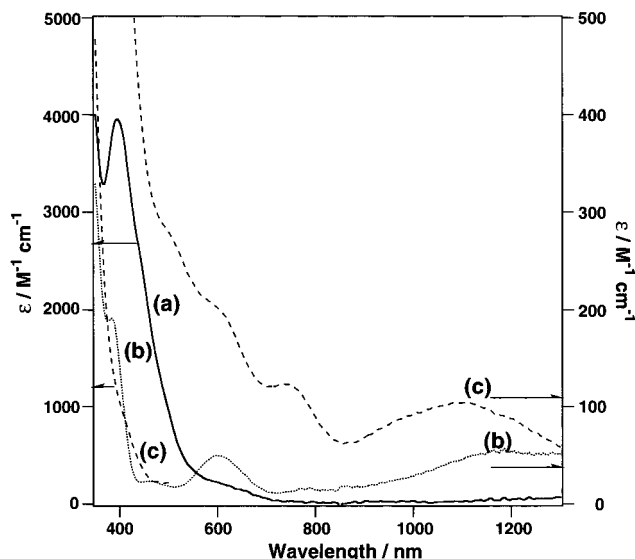
**Figure 4.** Electronic spectra of **1** (a) in acetone at −70 °C, **2** (b) in methanol at −50 °C, and **3** (c) in acetone at −50 °C.

**Spectroscopic Characterization of 1 and 3**. The electronic spectrum of **1** exhibits a distinct band at 394 nm ($\epsilon = \sim$4000 M$^{-1}$ cm$^{-1}$) in acetone at −70 °C (Figure 4), which is similar to that of **5** ($\lambda_{max}$ = 410 nm, $\epsilon$ = 4200 M$^{-1}$ cm$^{-1}$).[17] Based on the electronic spectrum together with the crystal structure, **1** can be assigned as a bis($\mu$-oxo)Ni$^{III}_2$ complex.

The ESI mass spectrum of **1** revealed that the dimer is preserved in MeOH at −78 °C. The positive-ion mass spectrum of **1** (X = ClO$_4$) in the range of $m/z$ 500 to 1500 shows a prominent signal at $m/z$ 913 (relative intensity ($I$) = 100%) with a characteristic distribution of isotopomers that matches well with the calculated isotopic distribution for $\{[Ni_2(O)_2(Me_3\text{-tpa})_2]\text{-}ClO_4\}^+$ (Figure 5a). The ESI mass spectrum of **1** generated by mixing a methanol solution of **2** (1 mM) with a methanol solution of 1 equiv of H$_2{}^{18}$O$_2$ at −78 °C revealed that no $^{18}$O was present in $\{[Ni_2(O)_2(Me_3\text{-tpa})_2]ClO_4\}^+$. A similar observation was made for **5**, where a rapid exchange of the oxo group by $^{16}$O in water occurred.[17]

The ESI mass spectrum of **3** in acetone at −78 °C did not exhibit a signal at $m/z$ 945 corresponding to $\{[Ni_2(O_2)_2\text{-}(Me_3\text{-tpa})_2]ClO_4\}^+$, but a signal at $m/z$ 422 ($I$ = 100%) corresponding to a monomeric species $[Ni(O_2)(Me_3\text{-tpa})]^+$ for $^{16}$O and at $m/z$ 426 for $^{18}$O (Figure 5b), suggesting that **3** can dissociate into monomer in acetone. However, there is a possibility that the monomer is formed only under the ESI mass conditions. Thus it is difficult to determine the solution structure of **3** (monomer or dimer) at present. During the decomposition process of **3**, the bis($\mu$-oxo)dinickel(III) species, ($\{[Ni_2(O)_2\text{-}(Me_3\text{-tpa})_2]ClO_4\}^+$; $I$ = 5%), was also detected, implying that **3** is converted into **1** during the decomposition process.

The resonance Raman spectrum of a powdered sample of **3** measured at ∼110 K shows an isotope-sensitive band at 1096 cm$^{-1}$ (1044 cm$^{-1}$ for an $^{18}$O-labeled sample prepared by H$_2{}^{18}$O$_2$) as seen in Figure 6. This value falls within the range characteristic for the O−O stretching vibrations for the superoxo-metal complexes.[39] The electronic spectrum **3** in acetone at −50 °C exhibits several d−d bands in the visible and near-infrared region, similar to those of distorted octahedral Ni(II) com-

(38) Niederhoffer, E. C.; Timmons, J. H.; Martell, A. E. *Chem. Rev.* **1984**, *84*, 137−203 and the references therein.
(39) Suzuki, M.; Ishiguro, T.; Kozuka, M.; Nakamoto, K. *Inorg. Chem.* **1981**, *20*, 1993−1996.
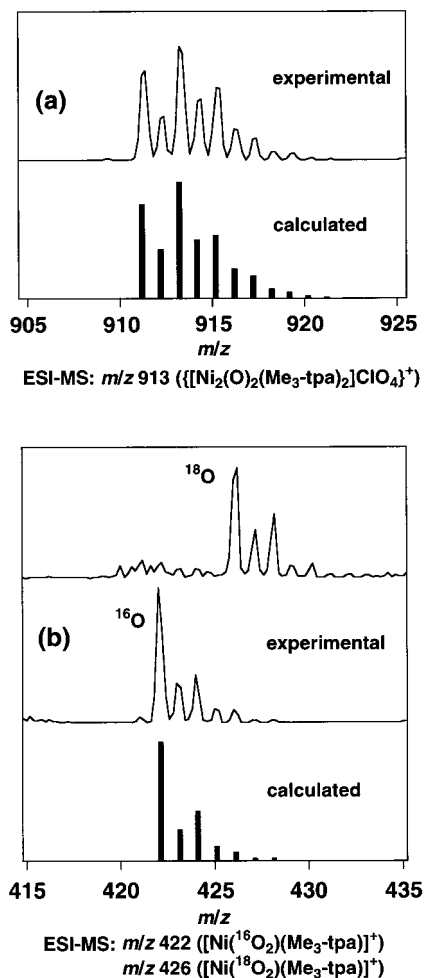
**Figure 5.** Electrospray ionization mass spectra of **1** (a) in MeOH and **3** (b) in acetone at −78 °C.
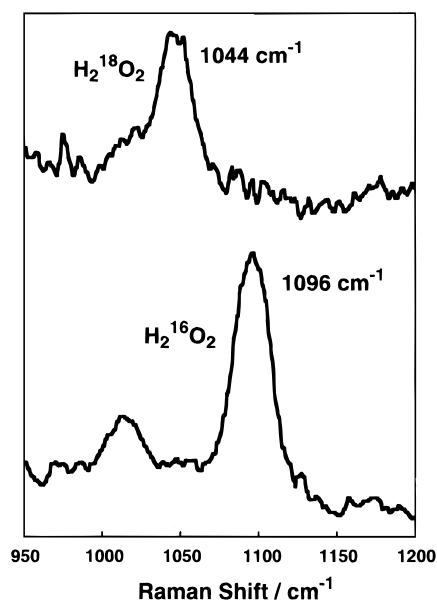


**Figure 6.** Resonance Raman spectra of a powdered sample of **3** at ~110 K obtained by using 488.0 nm laser excitation with 100 mW.

plexes,[40] although their intensities are stronger than those of **2** and some extra bands are observed (Figure 4).

(40) Lever, A. P. B. *Inorganic Electronic Spectroscopy*, 2nd ed.; Elsevier: Amsterdam, 1985.

**Reactivity of 1 and 3.** Thermal decomposition of **1** in acetone at −20 °C under $N_2$ atmosphere resulted in the hydroxylation of one of the methyl groups of $Me_3$-tpa to give (6-hydroxy-methyl-2-pyridylmethyl)bis(6-methyl-2-pyridylmethyl)amine ($Me_2$-tpaOH) in a yield of 24 ± 3%. A trace amount of N-dealkylated ligand, bis(6-methyl-2-pyridylmethyl)amine, and 6-methylpyridine-2-carbaldehyde were also detected by $^1$H NMR. Thus, the present bis($\mu$-oxo)Ni(III)$_2$ complex **1** has a regioselective monooxygenase activity for the coordinated ligand as found for bis($\mu$-oxo)Cu(III)$_2$ complexes,[5,9] a five-coordinate bis($\mu$-oxo)Ni(III)$_2$ complex **5**,[17] and a five-coordinate bis($\mu$-oxo)-Co(III)$_2$ complex **6**.[17] An isotope labeling experiment with $H_2^{18}O_2$ indicated that $Me_2$-tpaOH contains no $^{18}$O, which is consistent with the ESI-MS result described above. Thermal decomposition of **1** under $O_2$ in acetone at −20 °C gave a green powder within 2 h, which contains [Ni($Me_2$-tpaCOO)(OH$_2$)]$^+$ (**4**) identified by FAB-MS and X-ray structural analysis. The yield of $Me_2$-tpaCOO$^-$ recovered is 24 ± 3% along with $Me_2$-tpaOH (13 ± 2%). The FAB mass spectrum of a green powder obtained under $^{18}O_2$ atmosphere indicated that $Me_2$-tpaCOO$^-$ contains $Me_2$-tpaC$^{16}$O$^{16}$O$^-$ and $Me_2$-tpaC$^{16}$O$^{18}$O$^-$ in a 1:0.8 ratio, whereas $Me_2$-tpaC$^{18}$O$^{18}$O$^-$ was not identified. The result suggests that at least one of the carboxylate oxygens in $Me_2$-tpaCOO$^-$ comes from dioxygen, although significant scrambling occurred. Complex **1** is also capable for oxidizing external substrates, 2,4-di-*tert*-butylphenol to the corresponding biphenol almost quantitatively and triphenylphosphine (PPh$_3$) to PPh$_3$=O in yield of 40% determined by GC-MS.

Thermal decomposition of **3** in acetone at −20 °C under both $N_2$ and $O_2$ atmospheres also gave oxidized ligands. The yields of $Me_2$-tpaCOOH and $Me_2$-tpaOH under $O_2$ atmosphere are 25 ± 4% and 13 ± 2%, respectively. The result is similar to that for **1** under $O_2$ atmosphere. Interestingly, the thermal decomposition of **3** evolved dioxygen in a yield of 35 ± 4%. Complex **3** also oxidizes 2,4-di-*tert*-butylphenol to the corresponding biphenol. Preliminary decomposition kinetics of **3** in acetone, however, revealed that the addition of 2,4-di-*tert*-butylphenol does not affect the decomposition rate, but after decomposition, biphenol was produced almost quantitatively, where oxidation of ligand was not observed. The result implies that **3** itself cannot oxidize 2,4-di-*tert*-butylphenol.

## Discussion

The 6-methyl groups of the pyridyl sidearms have a significant influence on the formation and stabilization of high-valent bis($\mu$-oxo)dinickel(III) species as already mentioned. Note that only $Me_3$-tpa can stabilize the high-valent bis($\mu$-oxo)dinickel-(III) species and make its isolation possible. Although $Me_2$-tpa generated a brown species, its lifetime was within a few seconds, indicating that the presence of the three methyl groups is crucial for the stable formation of the high-valent bis($\mu$-oxo)dinickel-(III) species in the present ligand system. The space-filling model of **1** shown in Figure 7 reveals that the Ni$^{III}_2$($\mu$-O)$_2$ core is almost covered by a cavity formed by the three methyl groups of $Me_3$-tpa, which seems to be responsible for protecting the unstable Ni$^{III}_2$($\mu$-O)$_2$ core against some deleterious bimolecular decay pathways such as reactions with solvent molecules, disproportionation reaction between dimers through electron transfer, and so on.

The introduction of the 6-methyl group into the pyridyl sidearm causes a substantial elongation of the Ni−N bonds. It has been shown that the elongation of the M−N bonds weakens the electron donor ability of the pyridyl group, resulting in the destabilization of a higher oxidation state.[24a,25,32,33] This factor

*Bis(μ-oxo)nickel(III) and Bis(μ-superoxo)nickel(II) Complexes*

*J. Am. Chem. Soc., Vol. 122, No. 2, 2000* 261
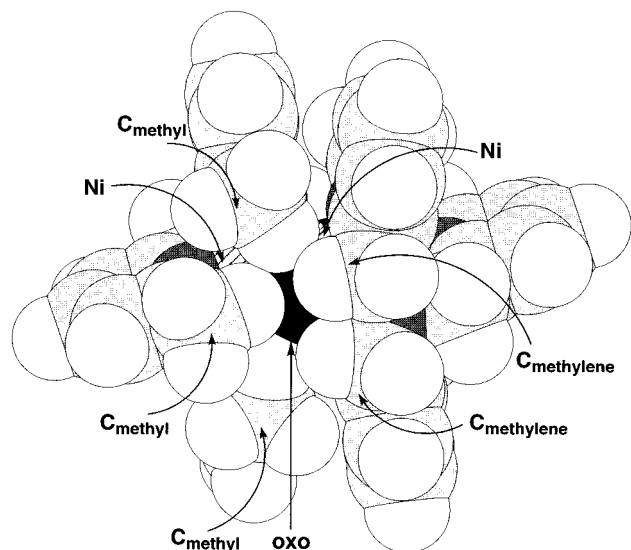


**Figure 7.** Space-filling view of **1** illustrating a $Ni^{III}_2(\mu\text{-}O)_2$ core surrounded by the $Me_3$-tpa moiety.

is unfavorable for the stabilization of a nickel(III) oxidation state, but the cavity formed by the three methyl groups seems to overcome this unfavorable effect and stabilize the $Ni^{III}_2(\mu\text{-}O)_2$ core in this system.

The ESI mass spectrum of **1** generated by $H_2^{18}O_2$ at $-78$ °C showed that $\{[Ni_2(O)_2(Me_3\text{-tpa})_2]ClO_4\}^+$ contained only $^{16}O$. This is probably due to a rapid exchange with water molecules present in the reaction mixture. Similar exchange reaction could proceed if an excess of hydrogen peroxide is present. In fact, **3** was obtained upon the addition of ca. 10-fold excess amount of $H_2O_2$ to **2**. Unfortunately, the ESI mass spectrum of **3** shows a signal at $m/z$ 422 ($m/z$ 426 for $^{18}O$) corresponding to a monomeric species $\{Ni(O_2)(Me_3\text{-tpa})\}^+$, the resonance Raman spectrum of **3** prepared with $H_2^{18}O_2$ under aerobic conditions provides the direct evidence that the superoxides come solely from hydrogen peroxide. While the substitution of two coordinated oxides in **1** by two peroxides followed by an electron transfer from $O_2^{2-}$ to Ni(III) readily explain the formation of **3**, we cannot exclude initial reduction of **1** by peroxide and the following ligand substitution by the resulting superoxide. In either case, **1** has enough redox potential for the oxidation of peroxide to superoxide. Similar redox reactions of peroxide have been proposed for the formation of a bis(μ-oxo)diiron(IV,IV) and the subsequent conversion into a bis(μ-oxo)diiron(III,IV) in the presence of hydrogen peroxide[16b] and for the formation of a superoxo dicopper(II) species generated by hydrogen peroxide.[41]

As already mentioned, **3** is not the active species responsible for the oxidation of 2,4-di-*tert*-butylphenol. In addition, thermal decomposition of **1** under $O_2$ atmosphere and that of **3** gave similar ligand oxidation, implying that an active species for the ligand oxidation in **3** is the bis(μ-oxo)Ni(III)$_2$ species, **1**. The formation of **1** was observed by the ESI mass spectrum of **3** upon thermal decomposition. Further, the dioxygen evolution upon thermal decomposition of **3** suggests one possible decomposition pathway of **3** to be a disproportionation of two coordinated superoxides to dioxygen and peroxide, followed by the O–O bond scission of peroxide to regenerate **1** (Scheme 1). Theopold et al. also have proposed that **8** decomposes to

(41) Kodera, M.; Tachi, Y.; Hirota, S.; Katayama, K.; Shimakoshi, H.; Kano, K.; Fujisawa, K.; Moro-oka, Y.; Naruta, Y.; Kitagawa, T. *Chem. Lett.* **1998**, 389–390.
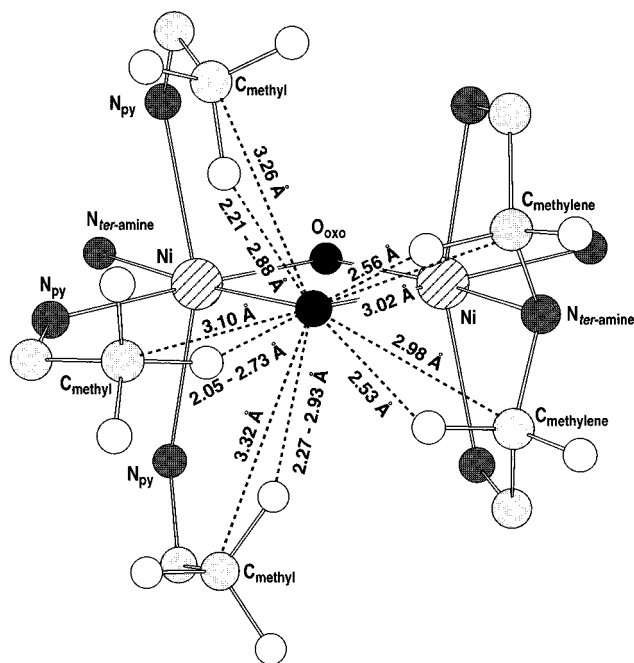


**Figure 8.** Chem3D view of **1** showing the $C\cdots O_{oxo}$ and $H\cdots O_{oxo}$ distances close to the oxo group. Hydrogen atoms were placed at the calculated positions. The C–H bond distances are set to 1.10 Å.

**Scheme 1.** Reaction Scheme of **1**, **2**, and **3**
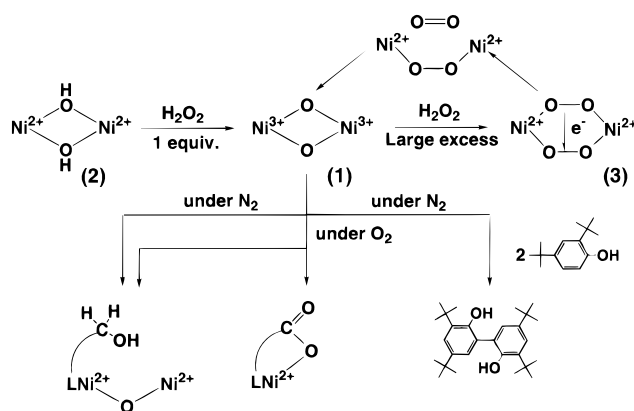


form a peroxo species, $[Co_2(O_2)(Tp^{iPr,Me})_2]$, with evolution of $O_2$, although the reaction has not yet been confirmed.[35]

The oxidation of the coordinated ligands in the high-valent bis(μ-oxo)dimetal(III) complexes is closely related to the structure and the C–H bond energy.[3b,7,9a,17] The regioselective oxidation of the methyl group in **1** is regulated by its own structure. The crystal structure of **1** reveals that the closest carbon atoms to the oxo group are the methylene carbon atoms of the 6-methyl-2-pyridylmethyl sidearms in the apical positions ($C\cdots O$ = 2.98 and 3.02 Å) as shown in Figure 8, whereas the distances between the oxygen atom of the oxo group and the 6-methyl carbon atoms in the equatorial position and in the axial positions are 3.10 and 3.26–3.32 Å, respectively. In $[Cu_2(O)_2$-$(Bn_3\text{-tacn})_2]^{2+}$ and $[Cu_2(O)_2(L_{ME})_2]^{2+}$, the distances between the oxo group and the carbon atoms on which the oxidation occurs are 2.79[3b] and 2.91 Å,[9] respectively. A Chem3D model suggested that the hydrogen atoms of the methyl groups, however, can approach more closely to the oxo group compared with those of the methylene carbon atoms of 6-methyl-2-pyridylmethyl sidearms in the apical positions, where the C–H bond distances are set to 1.10 Å. The distances of the H(methyl)$\cdots$O for the equatorial methyl group are 2.05–2.73 Å, and those

for the axial methyl groups are 2.21−2.93 Å depending on the orientation of the hydrogen atoms, whereas the distances of the H(methylene)···O are 2.56 and 2.53 Å. Thus the hydrogen atoms of the methyl group in the equatorial position can approach more closely to the oxo group. If the oxidation is initiated by the H-abstraction, this proximity effect seems to be responsible for the regioselective oxidation of the methyl carbon atom prior to that of the methylene carbon atom, although the H-abstraction from the methylene group is easier than that from the methyl group. Recently we found that thermal decomposition of a bis-($\mu$-oxo)Cu(III)$_2$ complex, $[Cu_2(O)_2(Me_2\text{-}tpa)_2]^{2+}$,[42] gave a regioselective *N*-dealkylated product of ligand, (6-methyl-2-pyridylmethyl)(2-pyridylmethyl)amine, where the oxidation occurs at the methylene carbon atom of the 6-methyl-2-pyridylmethyl sidearm in the apical position.

It is interesting that thermal decompositions of **1** under O$_2$ atmosphere and that of **3** under N$_2$ atmosphere produce Me$_2$-tpaCOO$^-$ together with the hydroxylated ligand, Me$_2$-tpaOH. There is a possibility that the hydroxymethyl group of Me$_2$-tpaOH could be oxidized by dioxygen in the presence of a metal ion, but the reaction of an acetone solution containing Me$_2$-tpaOH, 1 equiv of Ni(II) ion, and 1 equiv of *n*-Bu$_4$NOH under O$_2$ at −20 °C for 1 day (almost the same reaction conditions as those for the decomposition of **1** under O$_2$ atmosphere) did not give Me$_2$-tpaCOO$^-$, which was confirmed by FAB-MS. These results indicate that Me$_2$-tpaCOO$^-$ is not produced from the oxidation of Me$_2$-tpaOH by O$_2$. The reaction pathway for the formation of Me$_2$-tpaCOO$^-$ is not clear at present and currently under investigation.

In summary, a six-coordinate bis($\mu$-oxo)dinickel(III) complex **1** and a bis($\mu$-superoxo)nickel(II) complex **3** were synthesized for the first time and characterized by X-ray crystallography and various physicochemical techniques. The three 6-methyl groups of Me$_3$-tpa form a cavity around the bis($\mu$-oxo)dinickel-

(III) core that has a significant influence on the formation and stabilization of the bis($\mu$-oxo)dinickel(III) core at low temperature. Complex **3** was produced by the reaction of a bis($\mu$-oxo)nickel(III) complex **1** with a large excess of H$_2$O$_2$. This reaction demonstrates a unique conversion of a Ni$^{III}$($\mu$-O)$_2$Ni$^{III}$ core into a Ni$^{II}$($\mu$-OO)$_2$Ni$^{II}$ core upon exposure to hydrogen peroxide; **1** has enough redox potential for the oxidation of peroxide to superoxide. Decomposition of **3** is proposed to involve the disproportionation of two coordinated superoxides into dioxygen and peroxide followed by the O−O bond scission of peroxide to regenerate **1** which has a regioselective monooxygenase activity for a methyl group of the coordinated Me$_3$-tpa to give a hydroxylated ligand Me$_2$-tpaOH under N$_2$ atmosphere. In the presence of dioxygen, the oxidation of a methyl group to carboxylate also occurred, which is not produced from the oxidation of Me$_2$-tpaOH by dioxygen. The regioselective oxidation that occurred at the methyl carbon atom appears to be attributable to the proximity effect of the oxo group, which is initiated by hydrogen abstraction of the methyl group.

**Supporting Information Available:** Tables (S1−S16) listing crystallographic experimental details, final atomic coordinates, thermal parameters, and full bond distances and angles for **1**, **2**, **3**, and **4**, figures (S1−S4) displaying fully labeled ORTEP drawings for **1**, **2**, **3**, and **4,** and details of molar conductivity measurement (PDF). This material is available free of charge via the Internet at http://pubs.acs.org.

(42) Suzuki, M. et al. Submitted for pubulication.

JA990311D